# Characterisation of 3D trench sensors irradiated at FCC-hh fluences

- M. Verdoglia(1)(2), M. Addison(3), A. Bellora(4), F. Borgato(2), M. Boscardin(5),
- A. CARDINI<sup>(1)</sup>, G.M. COSSU<sup>(1)</sup>, G.F. DALLA BETTA<sup>(6)</sup>, L. LA DELFA<sup>(1)</sup>, A. LAI<sup>(1)</sup>,
- A. LAMPIS(1), A. LOI(1), M. OBERTINO(4), S. RONCHIN(5), and S. VECCHI(7)
- (1) INFN, Sezione di Cagliari Cagliari, Italy
- (2) Dipartimento di Fisica e Astronomia "Galileo Galilei", Università degli Studi di Padova -Padova, Italy
- (3) Department of Physics and Astronomy, University of Manchester Manchester, UK
- (4) Dipartimento di Scienze Agrarie, Forestali e Alimentari, Università degli Studi di Torino, Torino, Italy
- (5) Fondazione Bruno Kessler Trento, Italy
- (6) Dipartimento di Ingegneria Industriale, Università degli Studi di Trento Trento, Italy
- (7) INFN, Sezione di Ferrara Ferrara, Italy

Summary. — This contribution presents the latest measurements on extremely irradiated 3D-trench silicon sensors using the Transient Current Technique (TCT), performed at the INFN Cagliari laboratories. The 3D-trench sensors were developed within the INFN TimeSPOT project. TCT is used to assess the transport properties of electrons in silicon sensors. A sophisticated TCT setup has been built at INFN Laboratories in Cagliari to specifically study irradiated 3D-trench silicon pixel sensors in a low temperature environment. This setup is suitable for testing not only 3D-trench silicon sensor but also other silicon sensors, ASICs and small detectors (on the order of a few cm²). In the present paper, all the components of the setup are described, including both hardware and software, as well as the achieved results on extremely irradiated 3D-trench pixel sensors.

#### 1. - Introduction

Next-generation vertex detectors at colliders will be exposed to high levels of irradiation. In the case of FCC-hh the maximum radiation levels will reach values around  $10^{18}\,1\,MeV\,n_{eq}/cm^2$  [1]. To cope with the high luminosity, 4D tracking of the particles produced in collisions will be essential. This requires a precise measurement of the particles time of arrival on each detector layer. To assess the radiation hardness of innovative sensors that could be used for the new vertex detectors, several irradiation campaigns have been carried out over the years. In particular, the most recent one reached fluence

M. VERDOGLIA ETC.

levels of  $5\cdot 10^{17}$  and  $10^{18}\,1\,MeV\,n_{eq}/cm^2$  with neutrons provided by the Triga Mark II at Jožef Stefan Institute (JSI), exceeding those expected at the HL-LHC and approaching the levels foreseen for FCC-hh. The sensors chosen for these studies are the 3D-trench TimeSPOT silicon pixels [2] (fig. 1). TimeSPOT sensors are specifically designed to combine optimal timing performance with high radiation tolerance, achieved through a large collector anode and minimal spacing between the anode and the bias trenches. These sensors have already demonstrated a time resolution better than  $20\,ps$  under different irradiation levels from  $2.5\cdot 10^{16}\,1MeV\,n_{eq}/cm^2$  [3] up to  $10^{17}\,1MeV\,n_{eq}/cm^2$  [4].

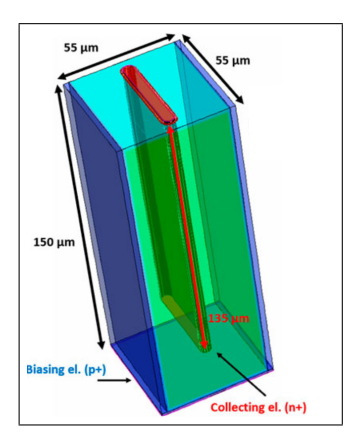


Fig. 1. - CAD model of a TimeSPOT 3D-trench silicon pixel sensor. (Image from [4]).

## 2. - Setup description

A schematic picture of the Cold-TCT setup is shown in fig. 2 (left). The cold-TCT setup employs a red laser  $(650 \, nm \text{ wavelength})$  and is compactly designed to minimize volume, allowing it to fit inside a climatic chamber. The climatic chamber used is a Weisstechnik<sup>TM</sup> model T180/70a/3, capable of reaching temperatures ranging from  $-70^{\circ}C$ to  $+180^{\circ}C$ . The chamber is equipped with two feedthroughs for signal and power cables, as well as for the laser's optical fiber. The driver used for the red or infrared lasers is a PicoQuant<sup>TM</sup> PDL 200-B, featuring a maximum pulse repetition rate of  $8\,MHz$ , and an electronic jitter of approximately 3 ps. A 650 nm laser with a 50 ps pulse width was used to investigate the surface properties of the sensors. The device under test (DUT) is mounted on three piezoelectric stages that allow movement along the x, y, and z axes, with travel ranges of  $48 \, mm$  in x and z, and  $16 \, mm$  in y. The z movement is used to focus the micrometric laser spot on the DUT, while the x-y movement is used to scan the DUT's active area (mapping). The front-end electronic is powered by a HAMEG™ HM7042-3 low-voltage power supply. A Keithley<sup>™</sup> model 6517A electrometer is used to supply reverse voltage to the sensors. A Rohde & Schwarz<sup>™</sup> model RTP 084 oscilloscope is used to acquire raw waveforms in the case of analog signal DUTs (fig. 2 right). The setup is mounted on a Thorlabs<sup>TM</sup> optical bench with dimensions of  $30 \times 30 \, cm^2$  and mechanical supports are used to achieve the best possible alignment. Other non-standard mechanical components used in the setup are 3D printed at the local INFN 3D Printing Lab in Cagliari. The optical bench is placed inside an RF-shielded box, which allows the system to be protected from light and radio-frequency sources. The laser can be

brought inside the climatic chamber via an optical fiber. At the fiber output, the beam is collimated by a triplet collimator and then focused by a  $2.5 \, mm$  focal-length lens to achieve a spot with an estimated micrometric diameter of about  $2-4 \, \mu m$ .

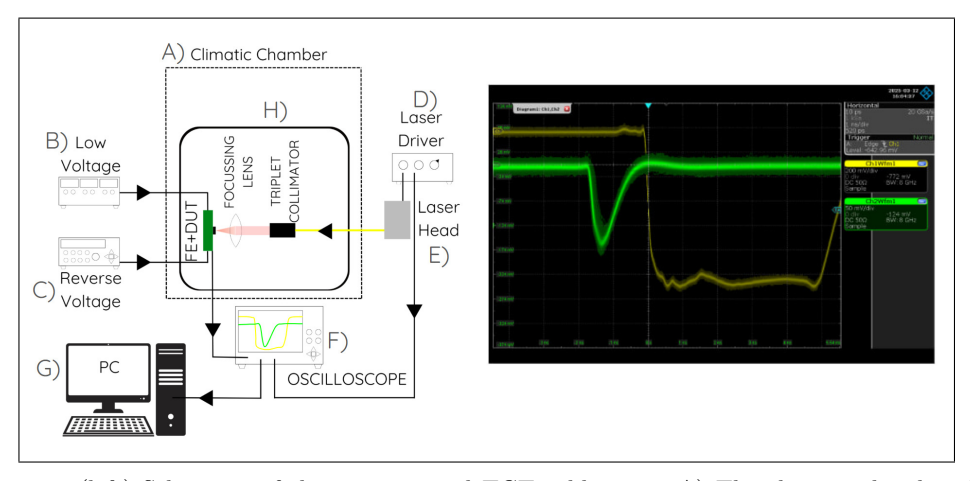


Fig. 2. – (left) Schematic of the experimental TCT cold setup. A) The climatic chamber, B) The low-voltage power supply, C) The electrometer/high-voltage power supply, D) The PDL driver, E) The laser head  $(650 \, nm)$ , F) The oscilloscope, G) The PC used for data control and acquisition. (right) Screenshot taken from the oscilloscope showing a typical set of raw waveforms generated in a non-irradiated 3D-trench pixel by the focused red laser  $(650 \, nm)$ .

#### 3. - Control software description

A PC is used to set all the parameters for data acquisition via a dedicated LabVIEW software specifically implemented for this task. The control software can handle all the described devices and allows to perform several measurements in series, automatically varying a single parameter each time. The main measurements consist of automatic scans in reverse voltage and temperature, not necessarily both simultaneously. The main feature of this setup is the XYZ piezoelectric stage system, which allows moving the DUT along the direction parallel to the laser beam to achieve the smallest possible laser spot, and then measuring the point performance of the DUT by moving it in micrometric steps across the plane perpendicular to the laser beam, covering the active area of the DUT.

## 4. - Signal amplitude measurements

By measuring the peak signal amplitude of each waveform for both non-irradiated and highly irradiated 3D-trench pixels, using a tuned laser set to  $100\,mV$  on the reference pixel, it is possible to compare the charge collection process, evaluate the charge collection efficiency (CCE), assess radiation damage, and ultimately determine the radiation tolerance of the sensors. The in-pixel amplitude maps corresponding to a non-irradiated pixel at  $100\,V$  bias voltage and a pixel irradiated at  $10^{17}\,1\,MeV\,n_{eq}/cm^2$  at  $300\,V$  bias voltage are shown in fig. 3 plots A) and B).

It can be observed that the irradiated sensor with increased voltage shows a recovery of the amplitude performance, approaching that of the non-irradiated reference. This

4 M. VERDOGLIA ETC.

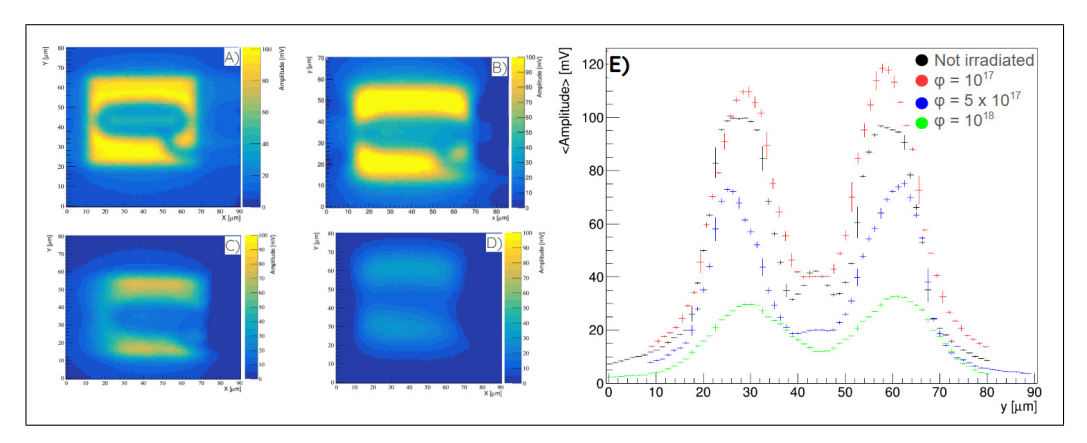


Fig. 3. – Amplitude maps measured using cold-TCT setup at  $T=-20^{\circ}C$ . A) Amplitude map of a non-irradiated 3D-trench TimeSPOT silicon pixel at  $50\,V$  bias voltage, with a fixed laser intensity for all measurements. B) Corresponding amplitude map of a pixel irradiated at  $10^{17}\,1\,MeV\,n_{eq}/cm^2$  at  $300\,V$  bias voltage. C) Corresponding amplitude map of a pixel irradiated at  $5\cdot10^{17}\,1\,MeV\,n_{eq}/cm^2$  at  $400\,V$  bias voltage. D) Corresponding amplitude map of a pixel irradiated at  $10^{18}\,1\,MeV\,n_{eq}/cm^2$  at  $400\,V$  bias voltage. E) Amplitude profiles showing the charge collection efficiency (CCE) relative to the reference pixel, which has a maximum amplitude of  $100\,mV$ .

measurement fully agrees with the results obtained in the previously conducted test beam campaign, where the MIP charge distribution MPV of a non-irradiated 3D-trench sensor was found to be equivalent to that of a pixel irradiated at  $10^{17} \, 1 MeV \, n_{eq}/cm^2$  [4]. Following the 2024 test-beam, a new irradiation campaign was conducted to reach fluences up to  $10^{18} \, 1 \, MeV \, n_{eq}/cm^2$ . The results of the cold-TCT measurements are shown in fig. 3 plot C) for a  $5 \cdot 10^{17} \, 1 \, MeV \, n_{eq}/cm^2$  irradiated sensor and D) for a  $10^{18} \, 1 \, MeV \, n_{eq}/cm^2$ . In order to compare the charge collection efficiency (CCE) of sensors irradiated at different levels, the one-dimensional amplitude distribution ( $1 \, \mu m$  resolution) along the central y-axis of the pixel was analysed. The results show that the pixel irradiated at  $10^{17} \, 1 \, MeV \, n_{eq}/cm^2$  and biased at  $300 \, V$  can recover and exhibits charge multiplication effects (as demonstrated at the test beam [4]). Using the cold-TCT setup the pixel irradiated at  $5 \cdot 10^{17} \, 1 \, MeV \, n_{eq}/cm^2$  biased at  $400 \, V$  can recover up to 70%, while the pixel irradiated at  $10^{18} \, 1 \, MeV \, n_{eq}/cm^2$  at the same bias voltage shows no significant recovery, with a maximum amplitude not exceeding 30%. A new front-end is currently in production, aiming to exceed the  $400 \, V$  bias limit and to enable performance evaluation of extremely irradiated sensors biased above  $400 \, V$ .

## 5. – Sub-Pixel temporal resolution measurements

It is of fundamental importance to evaluate the time of arrival of the laser signal on irradiated sensors. To achieve this, the raw waveforms collected using the cold-TCT setup are analyzed with a software Constant Fraction Discriminator (CFD) algorithm, which is used to calculate the Time of Arrival (TOA) of the signals, in reference to the time provided by the trigger (PDL-200), therefore, the TOA is obtained by subtracting the trigger TOA from the sensor TOA.

As in the case of the CCE study, it is also possible to reconstruct the in-pixel per-

formance maps shown on fig. 4 plots A),B) and C). Due to their low amplitude, the sensor irradiated at  $10^{18} \, 1 \, MeV \, n_{eq}/cm^2$  has been excluded from the analysis. Also in this case the measurements performed in laboratory using the cold-TCT setup, on  $10^{17} \, 1 \, MeV \, n_{eq}/cm^2$  irradiated test structures, are in good agreement with the results obtained at the test beam [4]. Of particular importance are the preliminary results obtained on 3D sensors irradiated up to  $5 \cdot 10^{17} \, 1 \, MeV \, n_{eq}/cm^2$ , which show a good temporal resolution ( $\sigma_t \sim 10 \, ps$ ). It is of fundamental importance to underline that the red 650 nm laser is only able to probe the surface due to its limited penetration depth. Therefore, even though the sub-pixel TOA plot in fig. 4, left, shows a reduction in the active area of extreme irradiated sensors, further studies are required to accurately characterize the efficiency. The compatibility with the temporal resolution of the non-irradiated reference sensor (fig. 4, right) can be fully validated once the efficiency is measured, for example in a test beam or by replacing the red 650 nm laser with an infrared laser at 1030 nm wavelength and illuminating the DUT from the back side, in order to avoid the metallization layers.

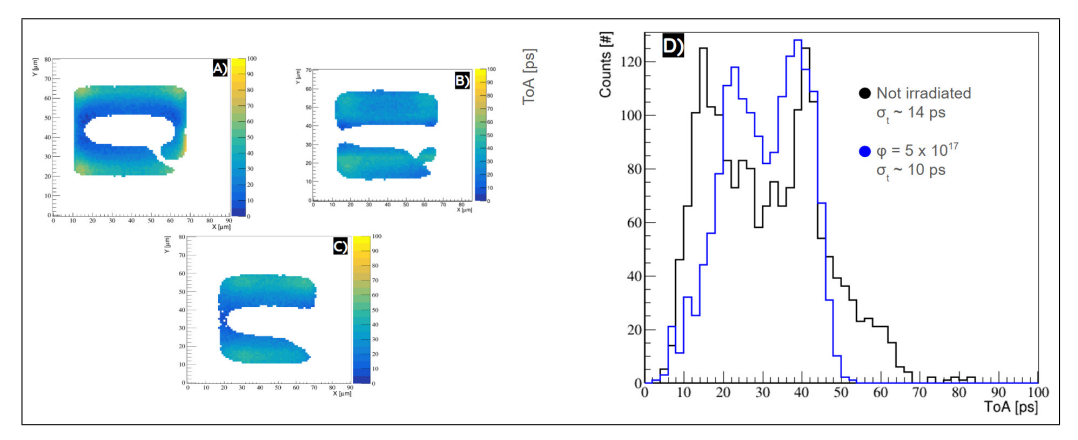


Fig. 4. – (left) TOA sub-pixel maps measured using cold-TCT setup at  $T=-20^{o}C$  applying an amplitude cut at half of the maximum amplitude. A) TOA map of a non-irradiated 3D-trench TimeSPOT silicon pixel at  $50\,V$  bias voltage, with the laser tuned at maximum amplitude of  $100\,mV$  and amplitude cut at  $50\,mV$ . B) Corresponding TOA map of a pixel irradiated at  $10^{17}\,1\,MeV\,n_{eq}/cm^2$  at  $300\,V$  bias voltage. C) Corresponding TOA map of a pixel irradiated at  $5\cdot10^{17}\,1\,MeV\,n_{eq}/cm^2$  at  $400\,V$  bias voltage. (right) D) TOA distributions for non-irradiated sensors and those irradiated up to  $5\cdot10^{17}\,1\,MeV\,n_{eq}/cm^2$  show no significant degradation in timing performance.

## 6. - Conclusions

In the present paper, the innovative Cold-TCT setup developed at the INFN laboratories in Cagliari is presented, demonstrating its capability to perform precise sub-pixel measurements of charge collection efficiency (CCE) and time resolution, consistent with the results obtained during a test beam campaign. The preliminary results show good performance of 3D-trench sensors irradiated up to  $5 \cdot 10^{17} \, 1 MeV \, n_{eq}/cm^2$ : the signal amplitude can be recovered up to 70%, and the timing capabilities remain compatible with those of the reference non-irradiated sensor; in fact, no degradation in performance has been observed. The test structures irradiated up to  $10^{18} \, 1 \, MeV \, n_{eq}/cm^2$  show a sig-

6 M. VERDOGLIA ETC.

nificant loss in signal amplitude. In fact, at a reverse bias of  $400\,V$ , the signal amplitude reaches only 30% compared to the non-irradiated reference.

Future studies aim to investigate extremely irradiated sensors up to  $10^{18} \, 1 \, MeV \, n_{eq}/cm^2$  using a modified front-end capable of exceed  $400 \, V$  of reverse bias voltage. Furthermore, an infrared  $1030 \, nm$  laser will be employed to mimic a MIP charge deposition, in order to investigate the sub-pixel bulk properties by illuminating the DUTs from the back side.

#### **Thanks**

Sensors irradiation founded by the European Union Grant Agreement No. 101057511. Many thanks to Igor Mandić (JSI) for taking care of the irradiation.

This work was supported by the Fifth Scientific Commission (CSN5) of the Italian National Institute for Nuclear Physics (INFN), within the Project TimeSPOT.

#### REFERENCES

- [1] ABADA, A. ET AL., The European Physical Journal Special Topics, (2019) FCC-hh: The Hadron Collider;
- [2] Loi A., https://hdl.handle.net/11584/284136, (2020) Design and test of a timing optimized 3D silicon sensor for HL-HLC experiments;
- [3] BORGATO, F. ET AL., Frontiers in Physics, 12 (2024) Characterisation of highly irradiated 3D trench silicon pixel sensors for 4D tracking with 10 ps timing accuracy;
- [4] Addison M., Frontiers in Physics, 12 (2024) Characterisation of 3D trench silicon pixel sensors irradiated at  $1 \cdot 10^{17} 1 \, MeV \, n_{eq} \, cm^2$ .